

## NUMERICAL SIMULATION OF HEAT-STORAGE PERFORMANCE OF FILLING BODY WITH UNIFORMLY MIXED PHASE CHANGE PARAFFIN

by

**Xiaoyan ZHANG<sup>a\*</sup>, Yaping KE<sup>a</sup>, Lang LIU<sup>a,b</sup>, Li LIU<sup>a</sup>,  
Ziyi HAN<sup>a</sup>, and Qingjiang LIU<sup>a</sup>**

<sup>a</sup> Xi'an University of Science and Technology, Xi'an, China

<sup>b</sup> Key Laboratory of Western Mines and Hazards Prevention, Ministry of Education of China,  
Xi'an, China

Original scientific paper  
<https://doi.org/10.2298/TSCI221231078Z>

*A PCM was added to filling materials in an appropriate proportion to realize the effective collection and storage of geothermal energy. Based on the theory of heat transfer and similarity, the heat-storage performance of filling body was numerically simulated in different states, then, the influences of paraffin proportion, initial temperature of filling body, surrounding rock temperature, stope air-flow temperature, and velocity on the heat-storage behavior of filling body were analyzed. The results revealed that reducing the initial heat-storage temperature of filling body, increasing surrounding rock temperature, and increasing the air-flow temperature in the stope all effectively increased the heat-storage capacity of filling body. In which the influence of initial temperature and surrounding rock temperature were more significant. At the end of 16 hours heat-storage period, when the initial temperature of filling body was reduced from 24 °C to 18 °C, the heat transfer capacity of filling body without paraffin and that with 5% paraffin decreased by  $2.85 \cdot 10^3$  kJ and  $2.40 \cdot 10^3$  kJ, respectively. When surrounding rock temperature increased from 35 °C to 45 °C, the amount of heat stored by two bodies increased by  $3.89 \cdot 10^3$  kJ and  $4.51 \cdot 10^3$  kJ, respectively.*

*Key words: paraffin, phase change, filling body, heat-storage performance, numerical simulation*

### Introduction

In recent years, mining technology has gradually developed to be more diverse and less destructive, and in consideration of applying mining engineering to deep stratum. To meet the needs of the stable and sustainable development of mineral enterprises, filling mining technology is necessary to enhance the safety of mining, improve the utilization rate of energy, and reduce the heat damage of mines [1, 2]. Therefore, the research of backfill mining technology, the rational exploitation and utilization of mine waste resources and geothermal resources, and the alleviation of mine thermal damage have attracted extensive attention of scholars at home and abroad. Zhu *et al.* [3] pumped low-cost filling materials with stable mechanical properties into goaf to realize safe and efficient mining. Ran [4] summarized the safety methods for mine filling. In order to solve the problems of thermal

\* Corresponding author, e-mail: zhangxy0629@xust.edu.cn

damage and solid waste in deep mines, Park *et al.* [5] reviewed the recent advancements in domestic mine recycling and the utilization of mine waste. Wang *et al.* [6] proposed a recycling economy model and filling body system for solid waste resource utilization to improve the energy recovery rate of mines. Wang *et al.* [7] proposed a novel method for deep mine cooling based on backfill containing PCM, and the results showed that the filling body containing PCM produced a clear cooling effect on stope. Guo *et al.* [8] proposed a mine geothermal cycle system for mine cooling and surface heating. Niu [9] employing a high-temperature mine as the research object, designed a system that integrated mine cooling and mine heat energy utilization.

In the filling mining, the selection of filling materials is very important for subsequent geothermal mining. Through the research in the field of building materials, it is found that the building materials with PCM can effectively reduce building energy consumption and realize energy conservation and environmental protection on the premise of maintaining the required strength of building walls, so their application research is very extensive [10], which also lays a foundation for the feasibility study of phase change filling body. Selvaraju *et al.* [11] introduced a novel concept of PCM effectiveness index to measure the thermal performance due to PCM integration in building. Kumar *et al.* [12] investigated the thermal properties of PCM in building walls through experimental tests. Li *et al.* [13] researched the effects of different parameters on the heat storage and release process of composite phase change wall. Cao *et al.* [14] integrated microcapsule PCM (MPCM) into geopolymer concrete, which can significantly improve the thermal performance of concrete.

Based on the advantages of high latent heat of PCM, it is technically feasible to add PCM into filling body for improving heat-storage performance in deep mine filling, when the filling body is also used as a structure supporting the underground stope space. Liu *et al.* [15] firstly proposed the application of PCM to mine to form functional filling body with heat storage/heat release. Liu *et al.* [16] developed a new type of PCM synthetic heat accumulator based on the huge latent heat of PCM. Wang *et al.* [17] studied the addition of ice into filling slurry for deep well cooling, and the heat transfer mechanism of ice-containing filling materials and ice through numerical simulation and experimental tests. Zhang *et al.* [18] studied the thermal and mechanical properties of ice filled filling body. Tan and Wang [19] conducted the experimental research on phase change latent heat materials to alleviate the mitigation of temperature change of mass concrete. Zhang *et al.* [20] analyzed the factors affecting the heat release process of filling body under the condition of deep mining stope, and obtained the influence mechanism of each factor on heat release performance and heat extraction rate.

By adding PCM to filling body to store geothermal energy by latent heat, the heat-storage performance can be effectively enhanced. There are different ways to add PCM to backfill, and the different ways have different effects on heat-storage performance. In terms of the study on the encapsulation of PCM with casing, Zhou *et al.* [21] analyzed the influence of Rayleigh number on the temperature field and flow field of wax in a circular tube. Zhang *et al.* [22] took the backfill body with tube-in-tube heat exchanger (PCM encapsulated in annular space) as research object and its heat-storage process and influencing factors is simulated and analyzed. In this study, the filling body is formed by adding different proportions of paraffin instead of filling aggregate under the condition that the filling material satisfied the necessary fluidity, structural stability and strength requirements. Additionally, based on heat transfer theory and similarity theory, the heat-storage process of filling body was investigated. The influence of the volume fraction of paraffin and the respective various factors, such as surrounding rock temperature, the initial temperature of filling body, the air-flow velocity and

air-flow temperature in stope, on the heat-storage performance of filling body were analyzed. The findings provide a theoretical reference for the study of heat collection and heat-storage for geothermal mining and the cooperative cooling of stope in deep mine.

### Model description

During heat-storage, the filling body absorbs heat from the surrounding rock and the air-flow of stope to increase its temperature. When the temperature reaches phase change temperature, paraffin will undergo a phase change, the filling body stores the heat as sensible heat or latent heat for geothermal energy exploitation. A schematic diagram and physical model of heat-storage process are respectively shown in figs. 1 and 2, and the model parameters are presented in tab. 1. The heat transfer between filling body and surrounding rock is a complex 3-D unsteady process. To simplify calculations, the following assumptions were made:

- Phase change filling body is a homogeneous, isotropic solid, and physical parameters remain constant, meaning that they are independent of temperature.
- Filling body is a porous medium in which the medium in the hole flows in a laminar state, and all phases are in a localized thermodynamic equilibrium.
- The respective influences of buried pipe and internal heat carrier are not significant when filling body is used for heat-storage.
- The PCM only occur solid-liquid phase change in a given temperature range, and are not susceptible to super-cooling or performance degradation.
- Natural convection does not occur when phase change occurs.
- The contact thermal resistance of tube wall is negligible.

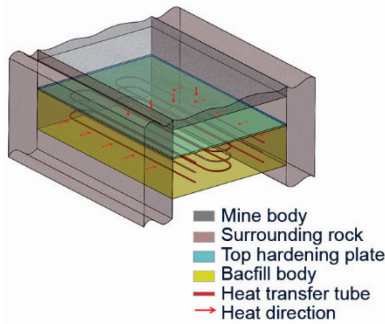


Figure 1. Schematic diagram for heat-storage of filling body

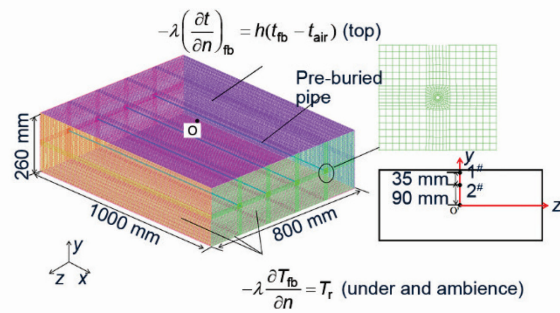


Figure 2. Physical model and grid division of filling body

Table 1. Physical property parameter

Name	Material	$\rho$ [ $\text{kg}\cdot\text{m}^{-3}$ ]	$C_p$ [ $\text{Jkg}^{-1}\text{K}^{-1}$ ]	$\lambda$ [ $\text{Wm}^{-1}\text{K}^{-1}$ ]	$L$ [ $\text{Jkg}^{-1}$ ]	$T_{\text{PCM}}$ [ $^{\circ}\text{C}$ ]
Pipe	PE	950	2100	0.46	–	–
PCM	RT28	Solid/liquid 860/790	Solid/liquid 1260 /2020	Solid/liquid 0.32/0.28	186000	Solid/liquid 26/28
Filling body	Cement mortar	1682	1650	0.6936	–	–

Structural tetrahedral and hexahedral grids were used for the mesh generation of model, the outer O-block method is used for the grid encryption of heat transfer tube. The pressure solver and the unsteady calculation method is adopted, the energy equation of laminar flow model and the melting solidification-porous medium model are opened. The finite volume method is adopted to improve the convergence velocity and calculation precision. Pressure coupler using SIMPLE, pressure, density and energy relaxation factor were 0.3, 1, and 1 respectively.

The heat-storage process with the grid number of about 0.825 million, 1.074 million, and 1.353 million and the calculation time steps of 5 seconds, 10 seconds, and 20 seconds for 16 hours was simulated. Tables 2 and 3 are the heat transfer capacity and the average temperature of filling body with different grid number and time steps at the heat-storage of 16 hours respectively. By comparing and analyzing the calculation results, it is more appropriate for the grid number of 1.074 million and the time steps of 10 seconds.

**Table 2. The change of the heat transfer capacity and average temperature of filling body with the number of grids**

Grid number [million]	Heat-storage capacity [ $1 \cdot 10^3$ kJ]	Average temperature [ $^{\circ}$ C]
0.825	9.101	34.184
1.074	9.104	34.319
1.353	9.113	34.469

**Table 3. The change of the heat transfer capacity and average temperature of filling body with the time steps**

Time step [seconds]	Heat-storage capacity [ $1 \cdot 10^3$ kJ]	Average temperature [ $^{\circ}$ C]
5	9.112	34.321
10	9.104	34.319
20	9.044	34.286

### *Mathematical model and thermal performance evaluation*

In this study, a 3-D model that simulates the heat-storage process of filling body has been established. The energy control equations of filling body with PCM and without PCM are shown in eqs. (1) and (2) respectively [23]:

$$\frac{\partial}{\partial \tau} \{ \varepsilon [\gamma \rho_l H_l + (1 - \gamma) \rho_s H_s] + (1 - \varepsilon) \rho_{fb} H_{fb} \} = \nabla (\lambda_{eff1} \nabla T) \quad (1)$$

$$\frac{\partial}{\partial \tau} [ \varepsilon \rho_{air} H_{air} + (1 - \varepsilon) \rho_{fb} H_{fb} ] = \nabla (\lambda_{eff2} \nabla T) \quad (2)$$

Equivalent thermal conductivity as follows:

$$\lambda_{eff1} = \varepsilon [\gamma \lambda_l + (1 - \gamma) \lambda_s] + (1 - \varepsilon) \lambda_{fb} \quad (3)$$

$$\lambda_{eff2} = \varepsilon \lambda_{air} + (1 - \varepsilon) \lambda_{fb} \quad (4)$$

The enthalpy-porosity method was used to analyze the phase transition in heat-storage process. This method is to treat the fuzzy region between liquid and solid phases

during phase change as the volume fraction of the porous region of liquid, without tracking the liquid phase interface [24]. For solidification and melting, the continuity equation is:

$$\frac{\partial \rho}{\partial t} + \nabla(\rho \vec{v}) = 0 \quad (5)$$

In this phase transition model, the enthalpy at any time can be calculated by sensible enthalpy  $h$  and latent enthalpy  $\Delta H$ :

$$H = h + \Delta H \quad (6)$$

$$h = h_{\text{ref}} + \int_{T_{\text{ref}}}^T C_p dT \quad (7)$$

The latent enthalpy is expressed as eq. (8):

$$\Delta H = \gamma L \quad (8)$$

The liquid fraction is expressed as eq. (9):

$$\gamma = \begin{cases} 1 & T > T_1 \\ \frac{T - T_s}{T_1 - T_s} & T_s < T < T_1 \\ 0 & T < T_s \end{cases} \quad (9)$$

The average temperature of filling body and the average liquid phase ratio of paraffin are used to calculate the total heat-storage capacity of each calculation region, which was denoted as:

$$Q = \sum_{j=1}^n \rho_{\text{fb}} c_{\text{fb}} V_{\text{fb}} (T_{i+1} - T_i) + \sum_{j=1}^n \rho_{\text{PCM}} c_{\text{PCM}} V_{\text{PCM}} (T'_{i+1} - T'_i) + \sum_{j=1}^n \rho_{\text{PCM}} c_{\text{PCM}} V_{\text{PCM}} (\gamma_{i+1} - \gamma_i) L \quad (10)$$

### Boundary conditions

It is assumed that the filling body is in a state of complete heat release when studying heat-storage process. That is to say, the initial temperature of heat-storage is equal to the temperature at the end of heat release:

$$T(x, y, z, \tau)|_{\tau=0} = T_{\text{int}} \quad (11)$$

The top of filling body is adjacent to stope, the heat transfer between filling body and the air-flow in stope is the third boundary condition:

$$-\lambda \left( \frac{\partial t}{\partial n} \right)_{\text{fb}} = h(T_{\text{fb}} - T_{\text{air}}) \quad (12)$$

The other walls of filling body is adjacent to surrounding rock, the wall temperature is equal to the temperature of surrounding rock:

$$T_w(x, y, z, \tau) = T_{\text{rock}} \quad (13)$$

### Thermal similarity model

Due to the actual filling body is relatively large, there are too many mesh nodes and the length width ratio is too large in filling body during the simulation, resulting in slow calculation, low calculation accuracy and poor simulation effect. Therefore, this simulation adopts the ratio of 1:10 between the simulation model and the actual model for similar transformation. The design parameters of similar model are shown in tab. 4. The principle of similarity transformation is expressed in literature [25].

**Table 4. Design parameters of similar model**

Design parameters	Prototype	Similar model
$B/W/H$ [mm]	10000/8000/2600	1000/800/260
$S$ [mm]	1600	160
$D$ [mm]	40	4
$T_{\text{int}}$ [°C]	18,21,24	18,21,24
$T_{\text{rock}}$ [°C]	35,40,45,	35,40,45,
$T_{\text{air}}$ [°C]	25,26,27	25,26,27
$v_{\text{air}}$ [ms <sup>-1</sup> ]	0.15,0.2,0.25	1.5,2.0,2.5
$t$ [h]	1600	16

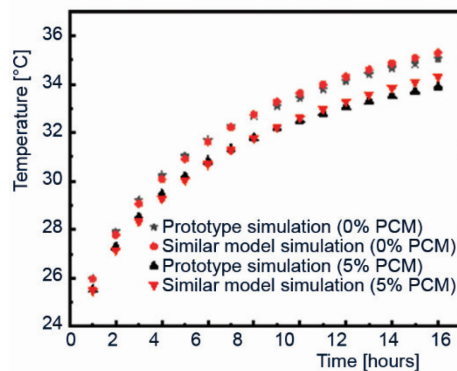


**Figure 3. Variation on average temperature of filling body**

simulation and prototype simulation is 2.08% for ordinary filling body and 1.26% for phase change filling body. The calculation of similar model can reflect the heat-storage process of filling body under actual working condition.

### Verification of filling body with uniformly mixed paraffin

For the filling body without paraffin, the accuracy verification of numerical model and simulation method was carried out by using the experimental results in [26]. The size of the verified model was 50 cm × 38 cm × 40 cm, the grid number was 960000 and the time

### Model validation

#### Verification of similar model

In order to verify the feasibility of similar transformation, the heat-storage process of the prototype model and the similar model of filling body were studied numerically on the condition that the boundary conditions were consistent. The grid number of similar model and prototype model is about 1.074 million and 1.628 million respectively, and the time steps is set as 10 seconds and 1000 seconds, respectively. Figure 3 shows the variation on average temperature of filling body with time under two models. It can be seen that the maximum relative error of similar

step was 10 seconds. The temperature of the center measuring point of filling body was selected as the comparison parameter and fig. 4(a) shows the comparison between the simulation results and the experimental results. The analysis shows that the simulation result is close to the experimental value and the maximum error is 6%. For the filling body with uniformly mixed paraffin, the simulation result was compared with the experimental results in [23]. The size of the verified model was 300 mm × 300 mm × 26 mm, the grid number was 264700 and the time step was 10 seconds. The internal face temperature of phase change wall was selected as the comparison parameter and fig. 4(b) shows the comparison between the simulation results and the experimental results. The analysis shows that the simulation results also are consistent with the experimental results and the maximum error is 3.37%. The two comparisons both effectively verified the accuracy and reliability of simulation method.

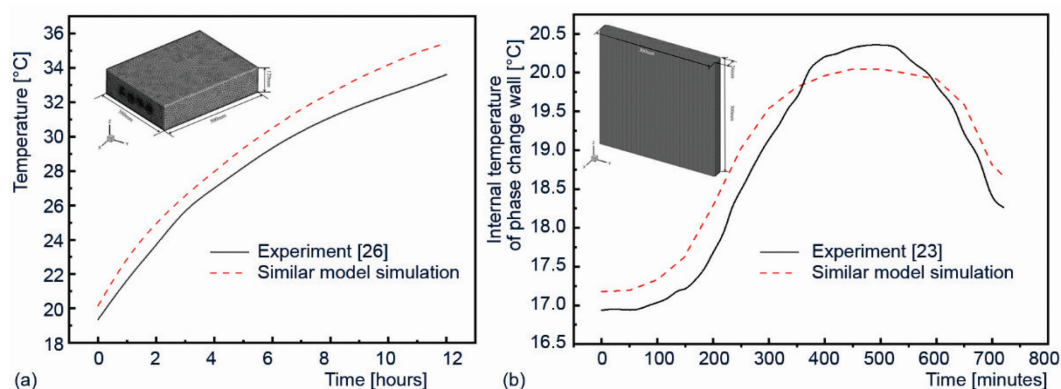


**Figure 4. Comparison between simulation results and experimental result;**  
**(a) the filling body without paraffin and (b) the filling body with uniformly mixed paraffin**

## Results and discussion

In this study, a filling body with 0%, 5% or 10% of paraffin microcapsules was utilized as the object. The influence of paraffin proportion on the heat-storage performance of filling body was analyzed. Additionally, the respective influences of the initial temperature of filling body, surrounding rock temperature and stope air-flow on the heat-storage performance of filling body were compared for the filling bodies with 0% (No. 1) and 5% (No. 2) paraffin.

### *Effects of paraffin proportion on the heat-storage performance of filling body*

The initial temperature of the filling body is 21 °C, the surrounding rock temperature is 40 °C, the air-flow temperature is 26 °C and the air-flow velocity is 2 m/s. Figure 5 shows the variations of the heat-storage parameters of filling body with time under different paraffin proportions. It can be seen from fig. 5(a) that the average temperature of filling body gradually increases with time and the increase rate of average temperature became lower and more gradual with the increasing of paraffin proportion. When the paraffin proportion increased from 0% to 5%, and 10%, the average temperature decreased from 35.31 °C to 34.32 °C and 33.84 °C, respectively, at the heat-storage of 16 hours, with the reductions of 0.99 °C and 1.47 °C. This is mainly because a higher proportion of paraffin results in more heat being stored in the form of latent heat, which can reduce the temperature of the filling body. Figure 5(b) shows that the liquid fraction of paraffin gradually increases with time.

When heat-storage duration is from 1-16 hours, the liquid fraction increased from 0.28 to 0.91 and from 0.26 to 0.87, respectively, for 5% and 10% paraffin added into the filling body. It also can be seen that a higher proportion of paraffin in filling body corresponds to a longer time required for the paraffin melting.

Figure 5(c) shows that the heat flux decreases with time and the decrease is obvious in the earlier stage. This mainly attributes to the increase of the high temperature region of the filling body in heat-storage process and the reduction of the heat transfer temperature difference between surrounding rock and filling body. In addition, the heat flux increased with paraffin proportion. When the paraffin proportion increased from 0% to 5% and 10%, the heat flux increased from  $12.25 \text{ W/m}^2$  to  $17.59 \text{ W/m}^2$  and  $19.74 \text{ W/m}^2$ , respectively, at the heat-storage of 16 hours, with the increases of  $5.07 \text{ W/m}^2$  and  $7.22 \text{ W/m}^2$ . A higher proportion of paraffin means that more heat can be stored in latent heat form, which decreases the temperature of the filling body and increases heat transfer temperature difference, so the heat flux also increases. Figure 5(d) shows that the heat-storage capacity of the filling body gradually increases with time and the increasing proportion of paraffin corresponds to a larger heat-storage capacity of the filling body. When the paraffin proportion increased from 0% to 5% and 10%, the heat-storage capacity increased from  $7.85 \cdot 10^3 \text{ kJ}$  to  $9.10 \cdot 10^3 \text{ kJ}$  and  $9.93 \cdot 10^3 \text{ kJ}$  respectively at the heat-storage of 16 hours, with the increases of  $1.25 \cdot 10^3 \text{ kJ}$

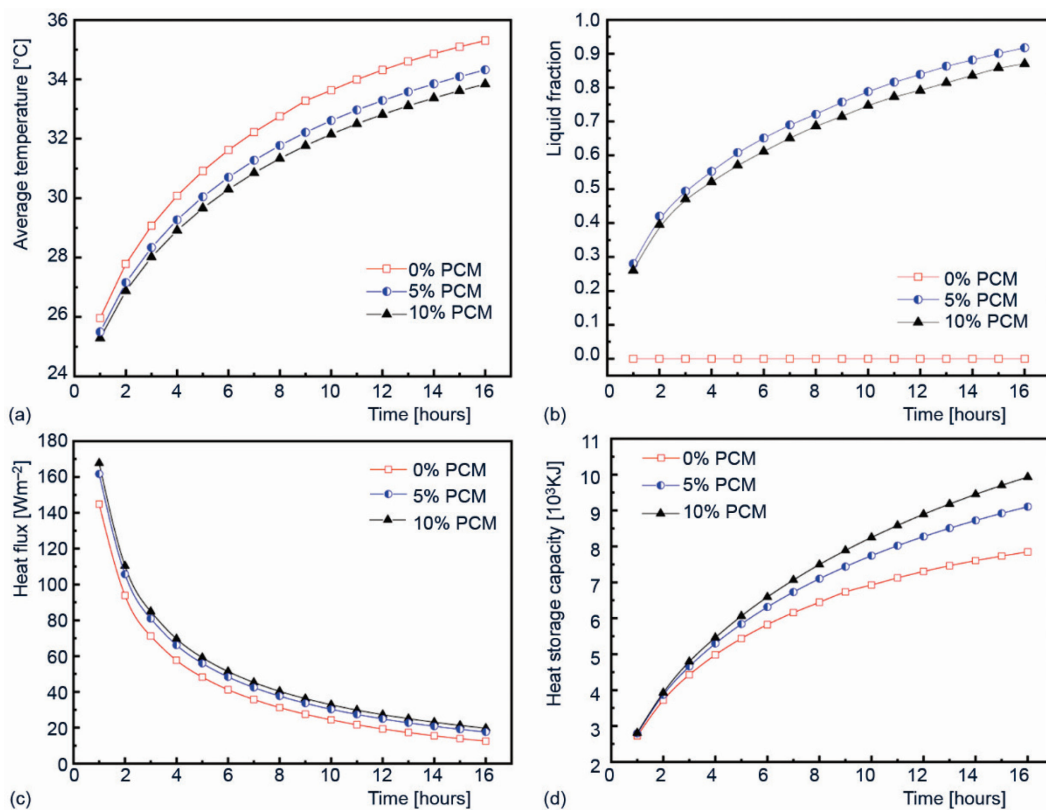


**Figure 5.** The variation in heat-storage parameters under different paraffin proportions; (a) average temperature of filling body, (b) liquid fraction of paraffin, (c) heat flux, and (d) heat-storage capacity

and  $1.08 \cdot 10^3$  kJ. This is mainly because, when the temperature of the filling body reaches the phase change temperature of paraffin, the heat-storage capacity includes not only the sensible heat of the filling body itself, but also a part of latent heat for the phase change of paraffin, so the higher the paraffin proportion, the greater the heat-storage capacity.

*Effects of initial temperature on the heat-storage performance of filling body*

The surrounding rock temperature is 40 °C, the air-flow temperature is 26 °C and the air-flow velocity is 2 m/s. The variations of the heat-storage parameters of filling body with time were analyzed and compared under different initial temperature of filling body. It can be seen from fig. 6(a) that the average temperature of filling body increases with the increase of initial temperature. When the initial temperature of filling body increased from 18 °C to 24 °C, the average temperature increments of No. 1 and No. 2 are 4.4 °C and 4.11 °C, respectively, at the heat-storage of 1 hour and are 0.86 °C and 0.79 °C, respectively, at the heat-storage of 16 hours. The data show that the difference of average temperature caused by the initial temperature change of filling body gradually decreases with the proceeding of heat-storage whether paraffin is added or not. According to fig. 6(b), the liquid fraction of paraffin also increases with the increase of initial

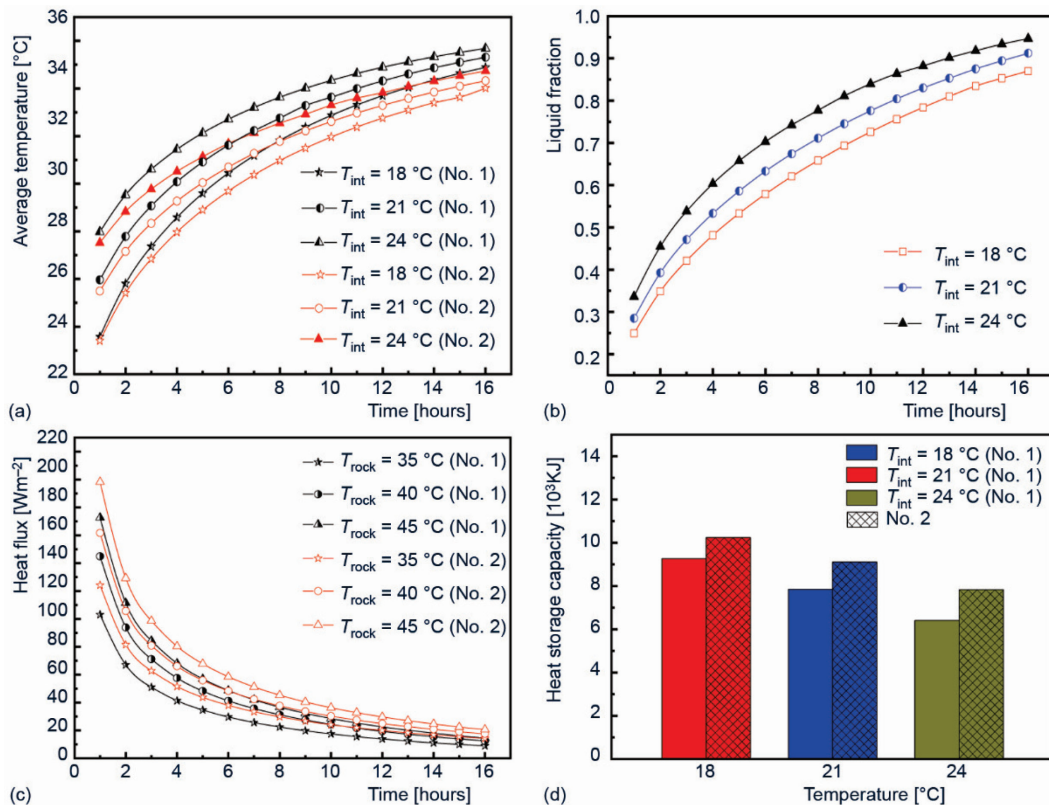


**Figure 6.** The variation in heat-storage parameters under different initial temperatures of filling body; (a) average temperature of filling body, (b) liquid fraction of paraffin, (c) heat flux, and (d) heat-storage capacity

temperature. When the initial temperature increased from 18 °C to 24 °C, the average increment of the liquid fraction is about 0.094 during the whole heat-storage period. This is because the increase of average temperature caused by the initial temperature of filling body accelerates the melting of paraffin.

Figure 6(c) shows that the heat flux decreases with the increasing of the initial temperature of the filling body. When the initial temperature of filling body increased from 18 °C to 24 °C, the heat flux decrements of No. 1 and No. 2 are 48.64 W/m<sup>2</sup> and 46.58 W/m<sup>2</sup>, respectively, at the heat-storage of 1 hour and are 4.63 W/m<sup>2</sup> and 5.61 W/m<sup>2</sup>, respectively, at the heat-storage of 16 hours. It is clear that the decrement of heat flux caused by the increase of the initial temperature of filling body obviously decreases with the proceeding of heat-storage whether paraffin is added or not. This rule is similar to the effect of initial temperature on the average temperature of the filling body. Figure 6(d) shows that the heat-storage capacity significantly decreases with the increase of the initial temperature of the filling body. When the initial temperature of the filling body increased from 18 °C to 24 °C, the heat-storage capacities of No. 1 and No. 2 decreased from 9.25 · 10<sup>3</sup> kJ to 6.40 · 10<sup>3</sup> kJ and from 10.23 · 10<sup>3</sup> kJ to 7.83 · 10<sup>3</sup> kJ, respectively, at the heat-storage of 16 hours, corresponding to the decrements of 2.85 · 10<sup>3</sup> kJ and 2.40 · 10<sup>3</sup> kJ. It is mainly because the increasing initial temperature reduces the temperature differences among the filling body, surrounding rock and the air-flow of slope, so the heat-storage capacity is reduced.

#### *Effects of surrounding rock temperature on the heat-storage performance of filling body*

The initial temperature of filling body is 21 °C, the air-flow temperature is 26 °C and the air-flow velocity is 2 m/s, fig. 7 shows the variations of the heat-storage parameters of filling body with time under different surrounding rock temperatures. As shown in fig. 7(a), the average temperature of filling body also increases with the increase of surrounding rock temperature. When the temperature of surrounding rock increased from 35 °C to 45 °C, the average temperature increments of No. 1 and No. 2 are 2.46 °C and 2.23 °C, respectively, at the heat-storage of 1 hour and are 7.1 °C and 6.96 °C, respectively, at the heat-storage of 16 hours. It is thus clear that the increment of the average temperature of filling body caused by the increase of surrounding rock temperature obviously increases with the proceeding of heat-storage. A higher surrounding rock temperature corresponds to a higher heat transfer rate from the surrounding rock to the interior of filling body, and also a higher heat transfer capacity, which causes a higher interior temperature of filling body. Figure 7(b) shows the liquid fraction of paraffin also increases with the surrounding rock temperature and the increase is more obvious when the surrounding rock temperature is from 35 °C to 40 °C. The average increment of liquid fraction is about 0.09 and 0.04, respectively, during the whole heat-storage period when the surrounding rock temperature increased from 35 °C to 40 °C and 45 °C.

Figure 7(c) shows that the heat flux increases with surrounding rock temperature and the increase is obvious in the earlier stage. When the surrounding rock temperature increased from 35 °C to 45 °C, the heat flux increments of No. 1 and No. 2 are 69.52 W/m<sup>2</sup> and 74.01 W/m<sup>2</sup>, respectively, at the heat-storage of 1 hour and are 5.58 W/m<sup>2</sup> and 6.38 W/m<sup>2</sup>, respectively, at the heat-storage of 16 hours. In the early stage, the heat transfer intensity between the surrounding rock and filling body is higher and the increasing surrounding rock temperature further increases the heat transfer intensity. However, with the proceeding of heat-storage, the decrease of heat transfer temperature difference weakens the heat transfer

intensity and the influence of surrounding rock temperature. Figure 7(d) shows that the heat-storage capacity of filling body obviously increases with the increase of surrounding rock temperature. When the surrounding rock temperature increased from 35 °C to 45 °C, the heat-storage capacities of No. 1 and No. 2 increased from  $5.89 \cdot 10^3$  kJ to  $9.78 \cdot 10^3$  and from  $6.79 \cdot 10^3$  kJ to  $11.30 \cdot 10^3$  kJ, respectively, at the heat-storage of 16 hours, corresponding to the increments of  $3.89 \cdot 10^3$  kJ and  $4.51 \cdot 10^3$  kJ. This is also due to the increase of heat transfer temperature difference caused by the increase of surrounding rock temperature.

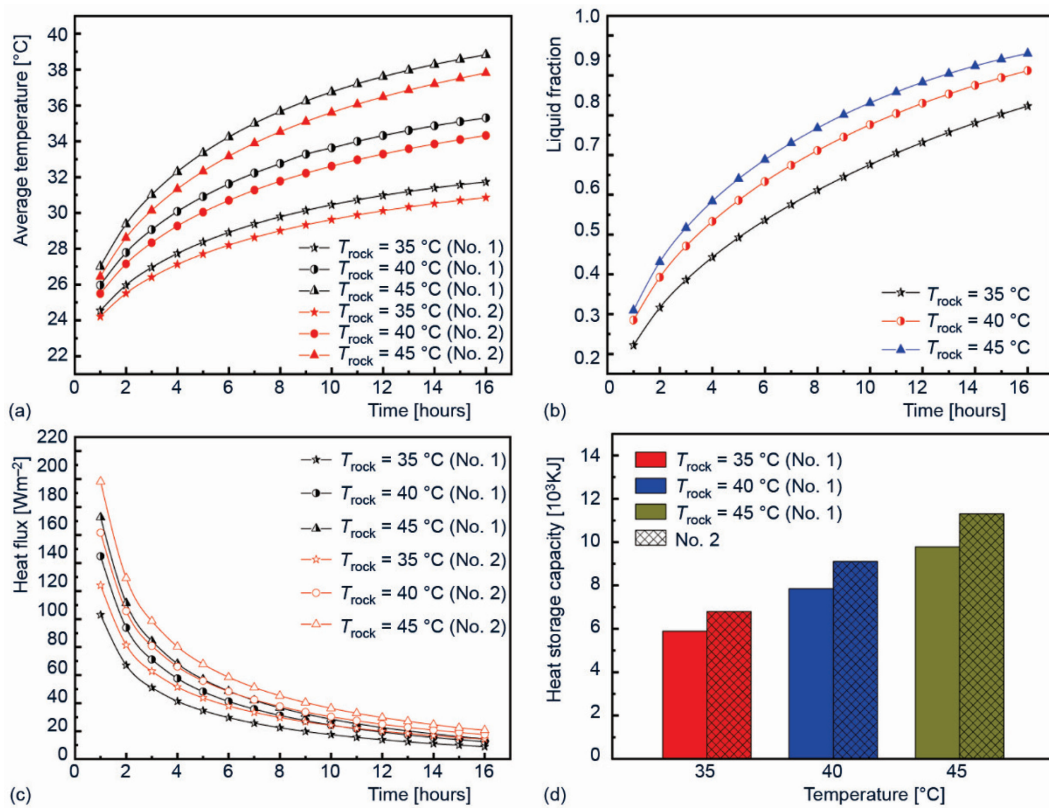


**Figure 7.** The variation in heat-storage parameters under different surrounding rock temperatures; (a) average temperature of filling body, (b) liquid fraction of paraffin, (c) heat flux, and (d) heat-storage capacity

#### *Effects of air-flow temperature and velocity on the heat-storage performance of filling body*

The initial temperature of filling body is 21 °C, the surrounding rock temperature is 40 °C and the air-flow velocity is 2 m/s, the influence of air-flow temperature (27 °C, 26 °C, and 28 °C) on the heat-storage performance of filling body was investigated. Figure 8(a) shows that the average temperature of filling body increases with the increase of air-flow temperature and the increment slightly increases with the proceeding of heat-storage. When the air-flow temperature increased from 24 °C to 28 °C, the average temperatures of No. 1 and No. 2 increased from 34.97 °C to 35.60 °C and from 34.08 °C to 34.55 °C, respectively,

at the heat-storage of 16 hours, corresponding to the increments of  $0.63\text{ }^{\circ}\text{C}$  and  $0.47\text{ }^{\circ}\text{C}$ . A comparison of the heat-storage capacity of filling body under different air-flow temperature is shown in fig. 8(b). It can be seen that, the heat transfer capacity of filling body also increases with the increase of air-flow temperature, but the increase is not noticeable.

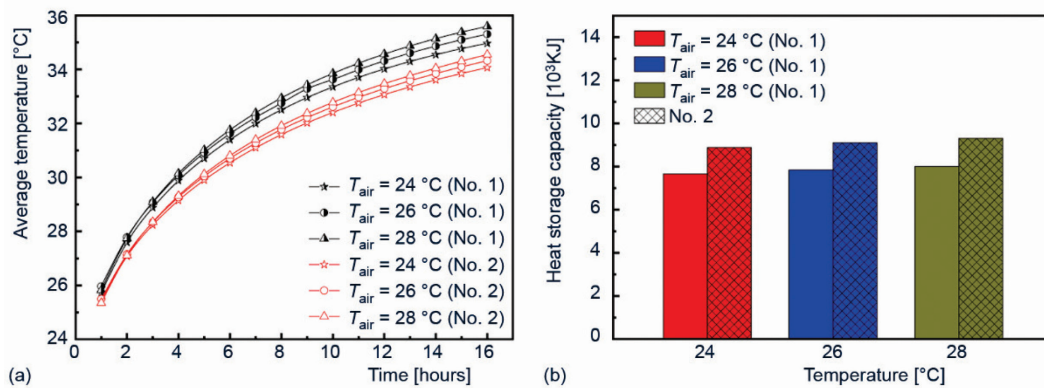


**Figure 8.** The variation in heat-storage parameters under different air-flow temperatures; (a) average temperature of filling body and (b) heat-storage capacity

To effectively investigate the influence of air-flow velocity on the temperature of filling body, the temperatures at monitoring points 1# and 2# (shown in fig. 2) were monitored under the condition of air-flow temperature of  $26\text{ }^{\circ}\text{C}$ . Figure 9 shows the temperature at each monitoring point changes with time. It can be seen that the temperature at each monitoring point slightly increases with the increase of air-flow velocity and this increase is even smaller in the late stage of heat-storage whether paraffin is added or not. This is mainly because that the selected monitoring points are close to the stope and far away from the surrounding rock, the heat transfer of surrounding rock did not reach the monitoring point in the early stage of heat-storage. So the influence of air-flow on the temperature at the monitoring point is more significant than that of the surrounding rock and a higher air-flow velocity corresponds to a higher heat transfer rate and a higher temperature at the monitoring points. With the

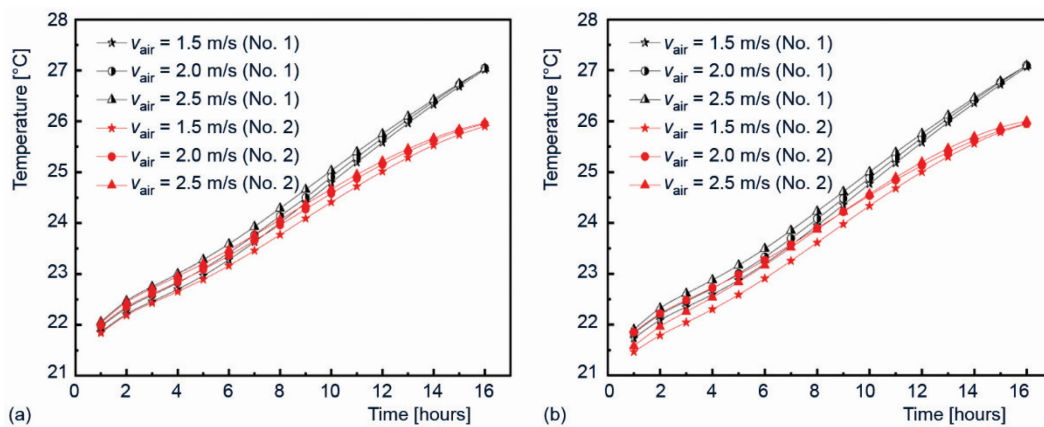


**Figure 9.** The variation in temperature at the measuring points during heat-storage process; (a) measuring point 1# and (b) measuring point 2#

proceeding of heat-storage, the heat of surrounding rock is gradually transferred to the interior of filling body, so the influence of heat transfer by surrounding rock on the temperature at the monitoring point gradually increases. This weakens the influence of heat transfer by air-flow, thus the temperature increase at the monitoring point caused by increasing air-flow velocity decreases in the later stage of heat-storage. Figure 10 shows the variation in the heat-storage capacity of filling body under different air-flow velocities. It can be seen that an increase in air-flow velocity has little effect on the heat-storage capacity of filling body.

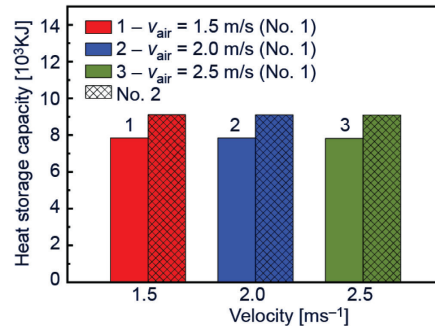


Figure 10. The variation in heat-storage capacity under different air-flow velocities

The initial temperature of filling body is 21 °C, the surrounding rock temperature is 40 °C, the air-flow temperature is 26 °C and the air-flow velocity is 2 m/s. To investigate the influence of heat transfer by surrounding rock and air-flow on the temperature of filling body, the distributions of the temperature field and the liquid fraction of paraffin in filling body of No. 2 were simulated during heat-storage. Figures 11 and 12 reveal that the temperature of filling body and the liquid fraction of paraffin both gradually increase from the surrounding rock boundary to the interior with the proceeding of heat-storage. It is thus clear that the heat transfer intensity between surrounding rock and filling body is obviously greater than that between filling body and air-flow in stope, that is, the heat transfer of surrounding rock is dominant in the process of heat-storage for filling body. This can also be well reflected from the comparison of the influence degree of surrounding rock temperature, air-flow temperature and velocity on the heat-storage capacity of filling body, as shown in figs. 7(d), 8(b), and 10.

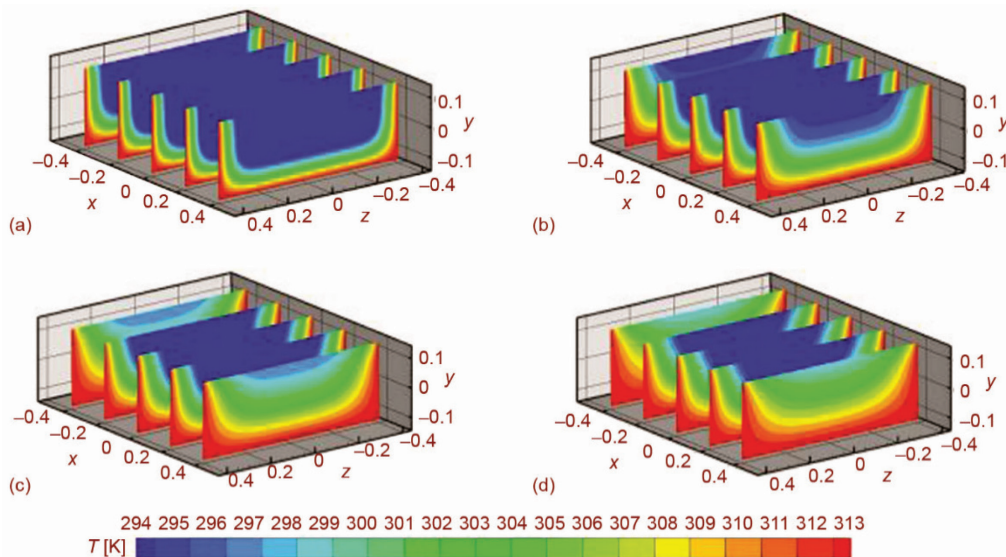
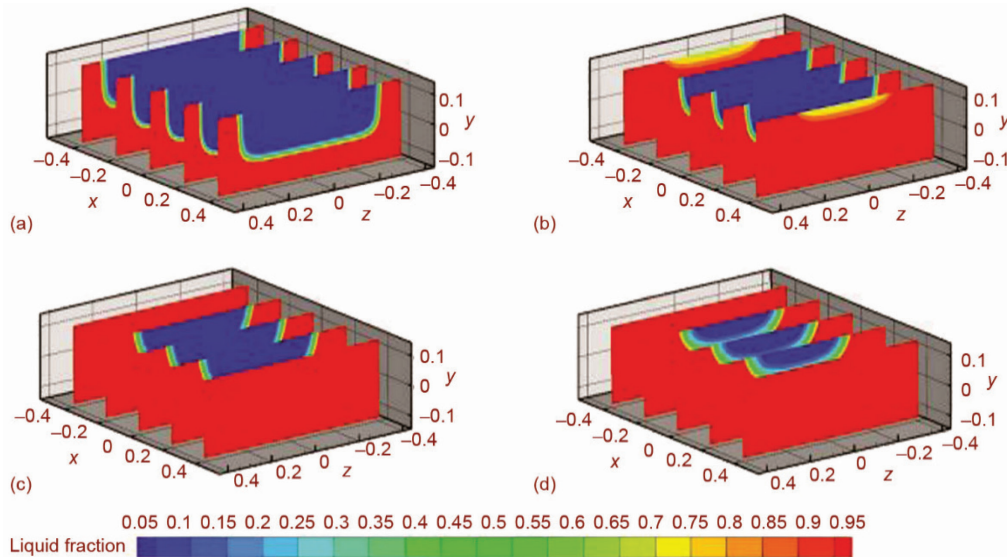


Figure 11. Distribution of temperature field in No. 2 during heat storage; (a)  $t = 4$  hours, (b)  $t = 8$  hours, (c)  $t = 12$  hours, and (d)  $t = 16$  hours



**Figure 12.** Distribution of liquid fraction of paraffin in No. 2 during heat-storage; (a)  $t = 4$  hours, (b)  $t = 8$  hours, (c)  $t = 12$  hours, and (d)  $t = 16$  hours

## Conclusions

In this study, the thermal behavior of filling body was numerically simulated under different proportions of paraffin and different heat transfer conditions, the main conclusions are as follows.

- With the increase of paraffin proportion, the average temperature of filling body obviously decreases while the heat-storage capacity increases significantly. Moreover, the difference of heat-storage capacity caused by different paraffin proportions becomes greater with the proceeding of heat-storage. The increment of heat-storage capacity is  $1.25 \cdot 10^3$  kJ and  $2.08 \cdot 10^3$  kJ for comparing paraffin proportion of 5% and 10% with that of 0% at the heat-storage of 16 hours.
- The average temperature of filling body increases while the heat-storage capacity significantly decreases with the increase of the initial temperature of filling body. When the initial temperature of filling body increases from 18 °C to 24 °C, the decrements of the heat-storage capacity of No. 1 and No. 2 are  $2.85 \cdot 10^3$  kJ and  $2.40 \cdot 10^3$  kJ, respectively, at the heat-storage of 16 hours.
- The average temperature and the heat-storage capacity of filling body both increase significantly with the increase of surrounding rock temperature. When the surrounding rock temperature increases from 35 °C to 45 °C, the increments of the heat-storage capacity of No. 1 and No. 2 are  $3.89 \cdot 10^3$  kJ and  $4.51 \cdot 10^3$  kJ, respectively, at the heat-storage of 16 hours.
- Compared with the influence of the initial temperature of filling body and the surrounding rock temperature on heat-storage process, the air-flow temperature and velocity have little effect on the heat-storage capacity of filling body. Compared with air-flow in stope, the heat transfer of surrounding rock is dominant in the process of heat-storage for filling body.

## Nomenclature

$B$  – length of the filling body, [mm]  
 $C_p$  – specific heat capacity, [ $\text{Jkg}^{-1}\text{K}^{-1}$ ]  
 $c_{\text{PCM}}$  – specific heat capacity of PCM, [ $\text{Jkg}^{-1}\text{K}^{-1}$ ]  
 $D$  – inner diameter of the prefabricated buried heat pipe [mm]  
 $h$  – sensible enthalpy, [ $\text{Jmol}^{-1}$ ]  
 $\Delta H$  – latent enthalpy, [ $\text{Jmol}^{-1}$ ]  
 $H$  – height of the filling body, [mm]  
 $L$  – latent heat, [ $\text{Jkg}^{-1}$ ]  
 $S$  – pipe spacing, [mm]  
 $T$  – temperature, [ $^{\circ}\text{C}$ ]  
 $T_{\text{PCM}}$  – temperature of solid and liquid of PCM, [ $^{\circ}\text{C}$ ]  
 $t$  – time, [h]  
 $\vec{v}$  – velocity vector, [ $\text{ms}^{-1}$ ]  
 $v$  – velocity, [ $\text{ms}^{-1}$ ]  
 $V$  – volume, [ $\text{mm}^3$ ]  
 $W$  – width of the filling body, [mm]

## Greek symbols

$\rho$  – density, [ $\text{kgm}^{-3}$ ]  
 $\lambda$  – thermal conductivity, [ $\text{Wm}^{-1}\text{K}^{-1}$ ]  
 $\varepsilon$  – porosity of porous  
 $\gamma$  – liquid fraction

## Superscript and subscripts

' – PCM  
eff – equivalent value  
fb – filling body  
 $i$  – certain time  
 $i+1$  – next moment  
int – initial value  
l – liquid phase  
ref – reference value  
rock – reference value  
s – solid phase  
w – wall

## Acknowledgment

This research was supported by the National Natural Science Foundation of China (Nos. 51974225, 52274063, 52004207, 52104148), Science and Technology Plan Project of Shaanxi Province (2022JM-173), Scientific Research Project of Youth Innovation Team Construction of Shaanxi Provincial Department of Education (No. 21JP077).

## References

- [1] Li, X., Liu, B., Review and Exploration of Current Situation of Backfill Mining in Hard Rock Mines, *Gold Science and Technology*, 26 (2018), 4, pp. 492-502
- [2] Dong, L., et al., Some Developments and New Insights of Environmental Problems and Deep Mining Strategy for Cleaner Production in Mines, *Journal of Cleaner Production*, 210 (2018), Feb., pp. 1562-1578
- [3] Zhu, J., et al., Research on the Technology of Filling and Repeated Mining in Thick Coal Seam Affected by Small Mine Gob Area, *Procedia Engineering*, 26 (2011), 05, pp. 1150-1156
- [4] Ran, J. J., Safe Mining Practices Under Wide Spans in Underground Non-Caving Mines – Case Studies, *International Journal of Mining Science and Technology*, 29 (2019), 4, pp. 535-540
- [5] Park, I., et al., A Review of Recent Strategies for Acid Mine Drainage Prevention and Mine Tailings Recycling, *Chemosphere*, 219 (2019), Mar., pp. 588-606
- [6] Wang, S., et al., Non-Explosive Mining and Waste Utilization for Achieving Green Mining in Underground Hard Rock Mine in China, *Transactions of Nonferrous Metals Society of China*, 29 (2019), 9, pp. 1914-1928
- [7] Wang, M., et al., Numerical and Experimental Studies on the Cooling Performance of Backfill Containing Phase Change Materials, *Building and Environment*, 218 (2022), 109155
- [8] Guo, P., et al., A Geothermal Recycling System for Cooling and Heating in Deep Mines, *Applied Thermal Engineering*, 116 (2017), Apr., pp. 833-839
- [9] Niu, Y., Research on Thermal Energy Recycling Utilization in High Temperature Mines, *Procedia Engineering*, 121 (2015), Dec., pp. 389-395
- [10] Xiao, L., Li, B., Research on Phase Change Materials in the Field of Building Energy Conservation, *Northern Architecture*, 4 (2019), 4, pp. 51-55
- [11] Selvaraju, A. P., et al., Thermal Management Analysis of PCM Integration In Building Using a Novel Performance Parameter - PCM Effectiveness Index, *Thermal Science*, 26 (2022), 2A, pp. 883-895

- [12] Kumar, S., *et al.*, Effect of Phase Change Material Integration in Clay Hollow Brick Composite in Building Envelope for Thermal Management of Energy Efficient Buildings, *Journal of Building physics*, 43 (2019), 4, pp. 351-364
- [13] Li, Y., *et al.*, Characteristics Optimization of Composite Phase change Wall During Intermittent Heating Process, *Science and Technology the Built Environment*, 26 (2020), 4, pp. 5411-551
- [14] Cao, V. D., *et al.*, Thermal Analysis of Multi-Layer Walls Containing Geopolymer Concrete and Phase Change Materials for Building Applications, *Energy*, 178 (2019), Nov., pp. 295-307
- [15] Liu, L., *et al.*, Basic Theories and Applied Exploration of Functional Backfill in Mines, *Journal of the China Coal Society*, 43 (2018), 7, pp. 1811-1820
- [16] Liu, Y., *et al.*, Experimental and Numerical Research on Development of Synthetic Heat Storage Form Incorporating Phase Change Materials to Protect Concrete in Cold Weather, *Renewable Energy*, 194 (2019), Apr., pp. 1424-1433
- [17] Wang, M., *et al.*, Cold Load and Storage Functional Filling Body for Cooling Deep Mine, *Advances in Civil Engineering*, 2018 (2018), 5435214
- [18] Zhang, X., *et al.*, Experimental Research on Heat Transfer and Strength Analysis of Backfill with Ice Grains in Deep Mines, *Sustainability*, 11 (2019), 9, 2486
- [19] Tan, Z., Wang, L., Experimental Study of Phase Change Latent Heat Materials to Mitigate Temperature Change of Mass Concrete, *Ready-Mixed Concrete*, 09 (2018), pp. 1-51
- [20] Zhang, X., *et al.*, Numerical Simulation of Heat Release Performance of Filling Body Under Condition of Heat Extracted by Fluid Flowing in Buried Tube, *Journal of Central South University*, 26 (2019), 8, pp. 2160-2174
- [21] Zhou, Z., *et al.*, Numerical Study on Nusselt Number of Moving Phase Interface During Wax Melting in Tube Using Lattice Boltzmann Method, *Thermal Science*, 26 (2022), 6B, pp. 4957-4967
- [22] Zhang, X., *et al.*, Numerical Simulation on Heat Storage Performance of Backfill Body Based on Tube-in-Tube Heat Exchanger, *Construction and Building Materials*, 265 (2020), 120340
- [23] Yan, H., Preparation and Application of Porous Matrix Phase Change Materials for Thermal Storage in Building Energy Conservation, Ph. D. thesis, Chongqing University, Chongqing, China, 2011
- [24] Buonomo, B., *et al.*, Numerical Study on Latent Thermal Energy Storage Systems with Aluminum Foam in Local Thermal Equilibrium, *Applied Thermal Engineering*, 159 (2019), 113980
- [25] Yang, S., Tao W., *Heat Transfer*, M. Higher Education Press, Oxford, UK, 2006
- [26] Zhang, X., *et al.*, Thermal-Mechanical Properties and Heat Transfer Process of Heat Storage/Energy Storage Backfill Body in Mine, *Journal of China Coal Society*, 46 (2021), 10, pp. 3158-3171